Publisher homepage: www.universepg.com, ISSN: 2663-6913 (Online) & 2663-6905 (Print)

https://doi.org/10.34104/ajpab.020.01040111

American Journal of Pure and Applied Biosciences

Journal homepage: www.universepg.com/journal/ajpab

Structure Prediction, Characterization, and Functional Annotation of Uncharacterized Protein BCRIVMBC126_02492 of *Bacillus cereus*: An *In Silico* Approach

Abu Saim Mohammad Saikat[1]*and Abul Bashar Ripon Khalipha[2,3]

[1]Dept. of Biochemistry and Molecular Biology, Bangabandhu Sheikh Mujibur Rahman Science and Technology University (BSMRSTU), Gopalganj, Bangladesh; [2]Dept. of Pharmacy, Bangabandhu Sheikh Mujibur Rahman Science and Technology University (BSMRSTU), Gopalganj, Bangladesh; [3]Evergreen Scientific Research Centre, Dept. of Pharmacy, Bangabandhu Sheikh Mujibur Rahman Science and Technology University (BSMRSTU), Gopalganj, Bangladesh.

*Correspondence: asmsaikat.bmb@gmail.com (Abu Saim Mohammad Saikat, Dept. of Biochemistry and Molecular Biology, BSMRSTU, Gopalganj, Bangladesh).

ABSTRACT

Bacillus cereus is enteropathogenic and widely distributed pathogen in the environment, which is mainly associated with food poisoning. In the intestine, *B. cereus* produces enterotoxins resulting in diarrhoea, abdominal distress and vomiting, and a range of infections in humans. BCRIVMBC126_02492 is a functional protein of *B. cereus,* which is related to oxidation glutathione persulfide in the mitochondria, cyanide fixation, and also has a variety of biological functions. Nevertheless, protein BCRIVMBC126_02492 is not explored. Therefore, the structure prediction, functional annotation, and characterization of the protein are proposed in this study. Modeller, Swiss-model, and Phyre2 are used for generating tertiary structures. The structural quality assessment of the protein determined by Ramachandran Plot analysis, Swiss-Model Interactive Workplace, and Verify 3D tools. Furthermore, Z-scores applied to detect the overall tertiary model quality of the protein. A comparison of the results showed that the models generated by Modeller were more suitable than Phyre2 and Swiss Models. This investigation decoded the role of this unexplored protein of *B. cereus*. Therefore, it can bolster the way for enriching our knowledge for pathogenesis and drug and vaccine targeting opportunities against *B. cereus* infection.

Keywords: *Bacillus cereus,* Protein BCRIVMBC126_02492, Functional annotation, and Pathogenesis.

1. INTRODUCTION

Bacillus cereus is omnipresent and a Gram-positive, spore-forming rod-shaped, non-capsulated, aerobic, or facultative anaerobic bacterium (Sankararaman and Velayuthan, 2013). The saprophytic life cycle of *B. cereus* is mainly in soil. Basedon 16S rRNA gene sequences, and it is closely related to other members in the *B. cereus* group, including *B. anthracis* and *B. thuringiensis* (Granum, 2017; Cui *et al.*, 2019). Generally, two types of food poisoning caused by *B. cereus,* such as the emetic poisoning appear 0.5-6 hours and the diarrheal syndromes poisoning appears 8-16 hours after the ingestion of contaminated food (Tallent *et al.*, 2015). *B. cereus* produces a potenttoxin-cereulide, which is a small, acid- and highly heat-resistant depsipeptide toxin resulting inthe food industries in several challenges (Rouzeau-Szynalski *et al.*, 2020). *B. cereus* causes the most side effects in

themicroecological preparations. The causes behind this are the overuse of antibiotics in animal feed and drug additives resulting in an unbalanced condition in the intestinal micro-ecosystems. This is also responsible for weakened immunity and drug resistance (Berthold-Pluta *et al*., 2015; Guo *et al.*, 2020). *B. cereus* inhibits the growthof detrimental bacteria and selectively pushes the activity of the microorganisms which live in the gastrointestinal tract (Riol *et al.*, 2018).

Additionally, *B. cereus* invigorates and boosts the growth of the host by producing advantageous metabolites (Raymond and Bonsall, 2013). The protein BCRIVMBC126_02492 present in *B. cereus* is associated with oxidation of glutathione persulfide to glutathione and persulfate in the mitochondria; cyanide fixation as well as other functions in biological systems. However, the tertiary structure with ligand binding active sites, physicochemical characterizations are not reported yet. Therefore, the tertiarystructures of the uncharacterized protein BCRIVMBC126_02492 with ligand binding active sites and functional annotations are propped in this study through an *in silico* approach.

2. MATERIALS AND METHODS

2.1 Sequence retrieval

The amino acid sequence of BCRIVMBC126_02492 obtained from the National Center for Biotechnology Information (NCBI) with the accession ID SCN08319.1. The 3D Structure is not available in the Protein Data Bank (PDB). As a result, the 478 amino acid long protein BCRIVMBC126_02492 present in *B. cereus* undertook for modeling secondary and tertiary structures, and for characterization and functional annotation as well.

2.2 Physicochemical characterization

We have used two web-based servers for the determination of the physicochemical properties of the uncharacterized protein. ProtParam tool applied for the prediction of instability and aliphatic index, amino acid composition, aliphatic index, and GRAVY (Gasteiger *et al.*, 2005). Besides, the Sequence Manipulation Suite (SMS) version 2 tool used for theoretical isoelectric point (pI) determination (Martin, Garrity and Yao, 2016).

2.3 Secondary structure prediction

The self-optimized prediction method with alignment (SOPMA) used for secondary structure elements prediction (Combet *et al.*, 2000)and the SPIPRED program (Jones, 1999) used to predict the secondary structure of BCRIVMBC126_02492. The DISOPRED tool used for disorder prediction (Thakur and Kumar, 2018).

2.4 Tertiary structure modeling and validation

The homology structure modeling of the protein BCRIVMBC126_02492 of *B. cereus* performed as there was no tertiary structure available in the Protein Data Bank (PDB). Three servers including Modeller (Webb and Sali, 2016) following the HHpred tool (Zimmermann *et al.*, 2018), Swiss-Model (Gasteiger *et al.*, 2005), and Phyre2 (Kelley *et al.*, 2015), used to predict the tertiary structures of the protein.The tertiary structures generated from Modeller, Swiss-Model, and Phyre2 compared. The most suitable tertiary structure selected for the final validation.For modeled tertiary structure validation, the Ramachandran plot analysis with PROCHECK and the Verify 3D (https://servicesn.mbi.ucla.edu/Verify3D/) followed. Also, the Swiss-Model Interactive Workplace (https://swissmodel.expasy.org/assess) applied for the final tertiary structure quality validation. Z-scores derived from the Prosa-web used for the overall tertiary model quality assessment experiment as well.

3. RESULTS AND DISCUSSION

3.1 Physicochemical characterization

The amino acid sequence of BCRIVMBC126_02492 present in *B. cereus* was retrieved in FASTA format and used as a query sequence for the determination of physicochemical parameters. The instability index of BCRIVMBC126_02492 is 34.60 (<40) indicates the stable nature of the protein (Guruprasad *et al*., 1990). The protein is acidic (pI 5.76, 6.04*), with a molecular weight of 54188.16 Da. High extinction coefficient values (64790) indicates the presence of Cys, Trp, and Tyr residues (Gill and von Hippel, 1989). Higher aliphatic index values (95.27) of the query protein

suggests as a decisive factor for increased thermos-stability for a wide temperature range. The protein is hydrophilic, and the possibility of better interaction with water (Uddin *et al*., 2017) as indicated by the lower grand average of hydropathicity (GRAVY) indices value (-0.256) as shown in **Table 1**. The amino acid composition showed in **Table 2**, which obtained from the ExPASy ProtParam Tool. The amino acid composition can help us to reveal the active amino acid pocket for drug and vaccine targeting against the protein.The uncharacterized protein has several functions, including it related to persulfide dioxygenase. This non-heme iron-dependent oxygenase catalyzes the oxidation of glutathione persulfide to glutathione and persulfide in the mitochondria as well as involved in a variety of biological functions (Sattler *et al.*, 2015). Also, it has a sulfide dehydrogenase enzymatic function. It plays a vital role in cyanide fixation and other features in biological systems as well as a variety of biological functions (Spallarossa *et al.*, 2001).

Table 1: Physicochemical parameters.

Physicochemical Parameters	Values
Number of amino acids	478
Molecular weight	54188.16
Theoretical isoelectric point (pI)	5.76, 6.04*
Aliphatic index	95.27
The instability index (II)	34.60
Extinction coefficient (all Cys from Cysteine)	64790
Extinction coefficients (all Cys reduced)	64290
Total number of negatively charged residues (Asp + Glu)	67
Total number of positively charged residues (Arg + Lys)	56
Grand average of hydropathicity (GRAVY)	-0.256

*pI determined by SMS Version2

Table 2: Amino acid composition.

S. No.	Amino Acids	Percentage (%)
1	Ala (A)	6.1
2	Arg (R)	3.1
3	Asn (N)	4.6
4	Asp (D)	6.5
5	Cys (C)	1.9
6	Gln (Q)	3.3
7	Glu (E)	7.5
8	Gly (G)	6.9
9	His (H)	2.9
10	Ile (I)	10.3
11	Leu (L)	8.6
12	Lys (K)	8.6
13	Met (M)	1.3
14	Phe (F)	4.2
15	Pro (P)	4.2
16	Ser (S)	4.8
17	Thr (T)	4.2
18	Trp (W)	1.3
19	Tyr (Y)	4.4
20	Val (V)	5.4

3.2 Secondary structure prediction

For the secondary structure prediction, the default setup (similarity threshold of 8, window width of 17, and the division factor of 4) was considered by SOPMA. By Utilizing 478 proteins (sub-database) and 33 aligned proteins, SOPMA predicted 39.54 percent of residues as random coils in comparison to alpha-helix (36.61 percent), extended strand (16.95 percent) and beta-turn of 6.90percent (**Table 3**). PSIPRED is showing the higher confidence of the prediction of the helix, strand, and coil (**Fig 1**).

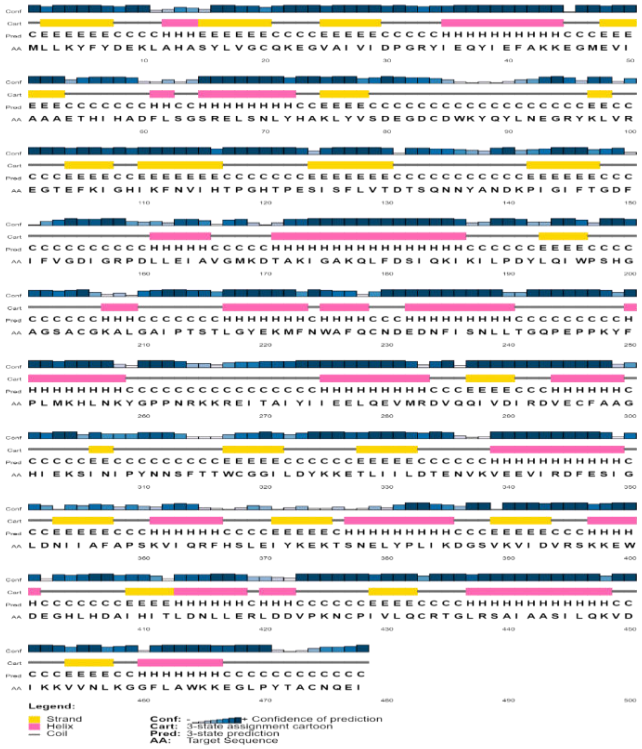

Fig 1: Predicted secondary structure.

Table 3: Secondary structure elements.

Secondary Structure Elements	Values (%)
Alpha helix (Hh)	36.61
3_{10} helix (Gg)	0.00
Pi helix (Ii)	0.00
Beta bridge (Bb)	0.00
Extended strand (Ee)	16.95
Beta turn (Tt)	6.90
Bend region (Ss)	0.00
Random coil (Cc)	39.54
Ambiguous states	0.00
Other states	0.00

3.3 Protein binding sites and Gene Ontology (GO) prediction

Predict protein server was applied for the determination of binding sites prediction where 12 different protein binding sites were identified at positions viz.: 4; 7-10; 88-89; 93-94; 134-138; 166; 259; 264-265; 267; 324; 326; 365, and 2 different polynucleotide binding sites were identified at positions viz. 434-435; 438. The macromolecule binding sites were found at nine different positions viz. 432; 433; 434; 435; 436; 437; 438; 438; and 440 (**Fig 2**). Gene ontology predicted and categorized the functional aspects of molecular functional ontology (**Table 4**), and biological process ontology (**Table 5**) and cellular component ontology (**Table 6**). Molecular functional ontology (**Table 4**) calculated as hydrolase activity (35%); thiol ester hydrolase activity (25%); hydrolase activity, acting on ester bonds (25%); hydroxyl acylglutathione hydrolase activity (25%); catalytic activity (23%); transition metal ion binding (16); binding (14%); ion binding (12%); and thiosulfate sulfurtransferase activity (11%). Biological process ontology (**Table 5**) detected as single-organism metabolic process (18%); single-organism process (18%); cellular process (18%); cellular metabolic process (18%); small-molecule biosynthetic process (17%); single-organism biosynthetic process (17%); peptide biosynthetic process (17%); nonribosomal peptide biosynthetic process (17%); oxoacid metabolic process (17%); and organonitrogen compound metabolic process (17%). Cellular component ontology (**Table 6**) predicted as cytoplasm (39%); cell part (39%); cell (39%); intracellular (39%); intracellular part (39%); intracellular organelle (17%); membrane-bounded organelle (17%); organelle (17%); mitochondrion (17%); and intracellular membrane-bounded organelle (17%).

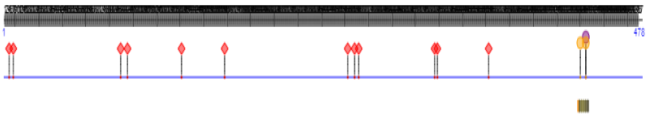

Fig 2: Protein-Protein and Protein-Polynucleotide binding sites.

Table 4: Molecular functional ontology.

GO ID	GO Term	Reliability (%)
GO:0016787	hydrolase activity	35
GO:0016790	thiolester hydrolase activity	25
GO:0016788	hydrolase activity, acting on ester bonds	25
GO:0004416	hydroxyacylglutathione hydrolase activity	25
GO:0003824	catalytic activity	23
GO:0046914	transition metal ion binding	16
GO:0008270	zinc ion binding	16
GO:0005488	binding	14
GO:0043167	ion binding	12
GO:0004792	thiosulfate sulfurtransferase activity	11

Table 5: Biological process ontology.

GO ID	GO Term	Reliability (%)
GO:0044710	single-organism metabolic process	18
GO:0044699	single-organism process	18
GO:0009987	cellular process	18
GO:0044237	cellular metabolic process	18
GO:0044283	small-molecule biosynthetic process	17
GO:0044711	single-organism biosynthetic process	17
GO:0043043	peptide biosynthetic process	17
GO:0019184	nonribosomal peptide biosynthetic process	17
GO:0043436	oxoacid metabolic process	17
GO:1901564	organonitrogen compound metabolic process	17

Table 6: Cellular component ontology.

GO ID	GO Term	Reliability (%)
GO:0005737	cytoplasm	39
GO:0044464	cell part	39
GO:0005623	cell	39
GO:0005622	intracellular	39
GO:0044424	intracellular part	39
GO:0043229	intracellular organelle	17
GO:0043227	membrane-bounded organelle	17
GO:0043226	organelle	17
GO:0005739	mitochondrion	17
GO:0043231	intracellular membrane-bounded organelle	17

3.4 Homology Modeling and Structural Validation

The target sequence of BCRIVMBC126_02492 in FASTA format inserted to HHpred Template Selection tool as input and the most active template was selected (3TP9_A) among the number of hits of 250 with the probability rate of 100 percent, E-Value of 6.7e-53, SS of 53.7, Cols of 462 and the target length of 474 (data not shown), and finally stored the tertiary modeled protein structure in PDB format predicted by Modeller (**Fig 3**). The tertiary structure assessment analyzation of the uncharacterized protein, the Ramachandran Map by PROCHECK (**Fig 4**) was used which shows that 92.6% of the total residues (387) were found in the core [A,B,L]; 6.0% of residues were in the additional allowed regions [a,b,l,p]; and there was 1.0% of residue were in the generously allowed regions [~a,~b,~l,~p] and 0.5% residue was in the disallowed regions. The number of non-glycine and non-proline residues was 418, which was 100%; the end-residues (excl. Gly and Pro) were 2; the glycine residues and proline residues were 33 and 20, respectively, among the total residues of 473 (**Table 7**). Verify 3D; a tertiary structure assessment tool was applied to show that the predicted tertiary Structure passed the assessment experiment (data are not shown). The Swiss-Model Interactive Workplace, another tertiary structure assessment tool, was used for the structure validation showing that the MolProbity Score was 3.25 and Ramachandran favored was 95.54% with the QMEAN (Qualitative Model Energy Analysis), Cβ, All Atom, solvation, and torsion values of -2.57, -2.45, -3.63, -0.43, -1.89, respectively (data are not shown).

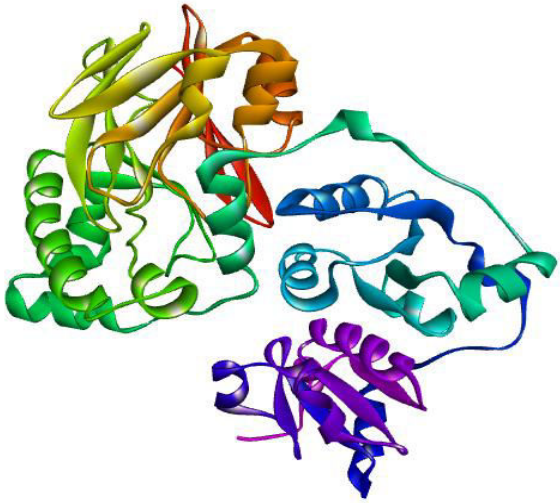

Fig 3: Structure of BCRIVMBC126_0249 predicted by Modeller.

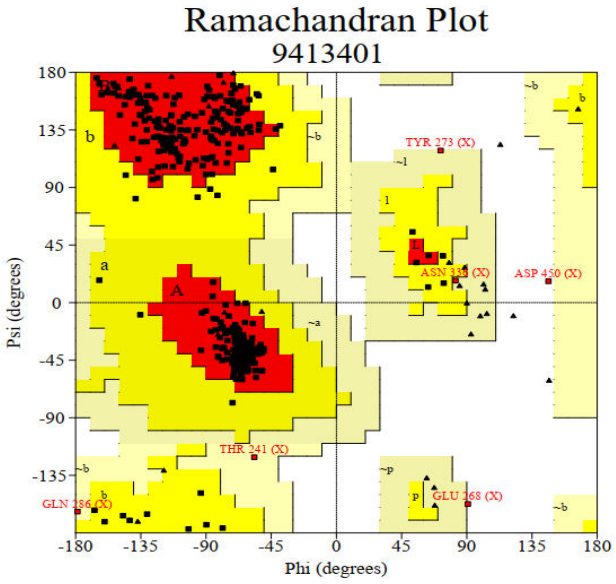

Fig 4: Ramachandran plot analysis.

Table 7: Ramachandran plot calculation.

Server	Ramachandran Plot Calculation	Value (%)
Modeller	Residues in most favored regions [A,B,L]	92.6
	Residues in additional allowed regions [a,b,l,p]	6.0
	Residues in generously allowed regions [~a,~b,~l,~p]	1.0

	Residues in disallowed regions	0.5
Phyre2	Residues in most favored regions [A,B,L]	91.3
	Residues in additional allowed regions [a,b,l,p]	7.2
	Residues in generously allowed regions [~a,~b,~l,~p]	1.2
	Residues in disallowed regions	0.2
Swiss Model	Residues in most favored regions [A,B,L]	91.9
	Residues in additional allowed regions [a,b,l,p]	7.4
	Residues in generously allowed regions [~a,~b,~l,~p]	0.4
	Residues in disallowed regions	0.4

Similarly, the tertiary model of BCRIVMBC 126_02492 performed with Phyre2 based on the most suitable template (c3tp9B_) with the value of confidence of 100.0% and coverage of 98%. The 467 residues (98% of the sequence) modeled with 100.0% confidence by the single highest scoring template with Phyre2. Phyre2 also described the secondary structure parameters as the disordered of 12%, alpha-helix of 32%, and beta-strand of 20% (data are not shown). Likewise, to analyze the tertiary structure assessment of the uncharacterized protein, Ramachandran Map by PROCHECK was used showing that 91.3% of the residues in most favored regions; 7.2% were in additional allowed regions; 0.2% were in disallowed regions, and there was 1.2% residue in the generously allowed regions (**Table 7**).

The predicted tertiary Structure gently passed the Verify 3D structure assessment experiment. The Swiss-Model Interactive Work place, another tertiary structure assessment tool, was used for the structure validation showing that the MolProbity Score was 2.81 and Ramachandran favored of 93.82%with the QMEAN, Cβ, all-atom, solvation, and torsion values of -2.36, -1.45, -2.61, 0.40, -2.21, respectively (data are not shown), thus, validating the predicted tertiary structure of the protein BCRIVMBC126_02492. The 3D model of BCRIVMBC126_02492also executed with Swiss-Modelbased on the top five suitable templates (3tp9.1.A; 3r2u.1.A; 3r2u.1.C; 3r2u.1.A; 3r2u.1.C), and the target sequence was selected based on the Qualitative Model Energy Analysis (QMEAN) score (-1.19), Global Model Quality Estimate (GMQE) score of 0.77, percentage of sequence identity of 45.06, and the coverage of 100%. The generated tertiary Structure stored in PDB format.Therefore, The tertiary structure assessment analyzation was performed by Ramachandran Map (PROCHECK) which showed 91.9% of the residues in most favored regions [A, B, L]; 7.4% were in additional allowed regions [a,b,l,p]; 0.4% were in disallowed regions, and 0.4% were in generously allowed regions (**Table 7**).

The modeled tertiary Structure passed the Verify 3D structure assessment experiment (data are not shown). The Swiss-Model Interactive Workplace, another tertiary structure assessment tool, was used for the structure validation showing that the MolProbity Score was 1.41 and Ramachandran favored of 94.05% with the QMEAN, Cβ, all-atom, solvation, and torsion values of -1.19, -0.54, -0.60, 0.46, -1.21, respectively (data are not shown) which validated the predicted 3D structure of the protein BCRIVMBC126_02492. The modeled structures of BCRIVMBC126_02492 were validated by another structure validation server, the Prosa-web (Wiederstein and Sippl, 2007). Standard bond angles in the shaped tertiary structures were determined by the Prosa-web, which performed to estimate the 'degree of nativeness' of the modeled tertiary structure. Z-scores for the tertiary structures predicted by the three servers, including Modeller, Swiss-Model, and Phyre2, were -10.39, -10.41, and -10.35, respectively. The Z-scored obtained from all three, e.g., Modeller, Swiss-Model, and Phyre2, are presenting similar values, thus, validating the predicted tertiary structures. The tertiary structure modeled by Modeller was more acceptable when compared to predicted structures by Phyre2, and Swiss Model. This comparison executed by following the Ramachandran Map analysis, Verify 3D results, Swiss-Model Interactive Workplace results, and by the z-scores analyzing.

4. CONCLUSION

In this study, it concluded that the structural model of the protein BCRIVMBC126_02492 with predicted active sites for ligand binding are useful for

understanding the protein nature. The physicochemical parameters prediction and functional annotation are useful for understanding the action of this protein's activity. The homology-modeled protein provides insights into the functional role of the protein BCRIVMBC126_02492 in pathogenesis which would help to design potential therapeutic drugs against the protein.

5. ACKNOWLEDGEMENTS

We are grateful to the Department of Biochemistry and Molecular Biology, and the Department of Pharmacy of Bangabandhu Sheikh Mujibur Rahman Science and Technology University, Gopalganj, Bangladesh, for supporting this study.

6. CONFLICTS OF INTETEST

The authors declare no conflict of interest.

7. REFERENCES

1. Berthold-Pluta, A., Pluta, A. and Garbowska, M. (2015). 'The effect of selected factors on the survival of *B. cereus* in the human gastrointestinal tract', *Microbial Pathogenesis*. Elsevier Ltd, **82**, pp. 7-14. https://doi.org/10.1016/j.micpath.2015.03.015
2. Combet, C. *et al.* (2000). 'NPS@: Network protein sequence analysis', *Trends in Biochemical Sciences*. Elsevier Ltd, pp. 147-150. https://doi.org/10.1016/S0968-0004(99)01540-6
3. Cui, Y. *et al.* (2019). 'Multifaceted toxin profile, an approach toward a better understanding of probiotic *Bacillus cereus*', *Critical Reviews in Toxicology*. Taylor & Francis, **49**(4), pp. 342-356. https://doi.org/10.1080/10408444.2019.1609410
4. Ekhlas Md. Uddin, Maitra Pulak, Hossain Md. Faruquee, Alam Md. Firoz, (2014). Isolation and characterization of proteases enzyme from locally isolated *Bacillus sp*., *American J. of Life Sciences*. **2**(6), 338-344. https://doi.org/10.11648/j.ajls.20140206.12
5. Gasteiger, E. *et al.* (2005). 'Protein Identification and Analysis Tools on the ExPASy Server', in *The Proteomics Protocols Handbook*. Humana Press, pp. 571-607. https://doi.org/10.1385/1-59259-890-0:571
6. Gill, S. C. and von Hippel, P. H. (1989). 'Calculation of protein extinction coefficients from amino acid sequence data', *Analytical Biochemistry*. Academic Press, **182**(2), pp. 319-326. https://doi.org/10.1016/0003-2697(89)90602-7
7. Granum, P. E. (2017). 'Spotlight on *Bacillus cereus* and its food poisoning toxins', *FEMS Microbiology Letters*, **364**(10), pp. 1-3. https://doi.org/10.1093/femsle/fnx071
8. Guo, R. *et al.* (2020). 'Biological characteristics and genetic evolutionary analysis of emerging pathogenic *Bacillus cereus* isolated from Père David's deer (*Elaphurus davidianus*)', *Microbial Pathogenesis*. Elsevier Ltd, **143**, p. 104133. https://doi.org/10.1016/j.micpath.2020.104133
9. Guruprasad, K., Reddy, B. V. B. and Pandit, M. W. (1990). 'Correlation between stability of a protein and its dipeptide composition: a novel approach for predicting in vivo stability of a protein from its primary sequence', *Protein Engineering, Design and Selection*. *Oxford Academic*, **4**(2), pp. 155-161. https://doi.org/10.1093/protein/4.2.155
10. Jones, D. T. (1999). 'Protein secondary structure prediction based on position-specific scoring matrices', *Journal of Molecular Biology*. Academic Press, **292**(2), pp. 195-202. https://doi.org/10.1006/jmbi.1999.3091
11. Kelley, L. A. *et al.* (2015). 'The Phyre2 web portal for protein modeling, prediction and analysis', *Nature Protocols*. Nature Publishing Group, **10**(6), pp. 845-858. https://doi.org/10.1038/nprot.2015.053
12. Martin, L., Garrity, D. M. and Yao, T. (2016). Genomics and transcriptomics of the molting gland (Y-organ) in the blackback land crab, *Gecarcinus lateralis*. Colorado State University. Libraries.
13. Raymond, B. and Bonsall, M. B. (2013). 'Cooperation and the evolutionary ecology of bacterial virulence: The *Bacillus cereus* group as a novel study system', *Bio Essays*, **35**(8), pp. 706-716. https://doi.org/10.1002/bies.201300028
14. Riol, C. Da *et al.* (2018). 'Consumed foodstuffs have a crucial impact on the toxic activity of Enteropathogenic *Bacillus cereus*', *Frontiers in Microbiology*, **9**, pp. 1-10. https://doi.org/10.3389/fmicb.2018.01946

15. Rouzeau-Szynalski, K. *et al.* (2020). 'Why be serious about emetic *Bacillus cereus*: Cereulide production and industrial challenges', *Food Microbiology*. Elsevier Ltd, **85**, p. 103279. https://doi.org/10.1016/j.fm.2019.103279
16. Sankararaman, S. and Velayuthan, S. (2013). '*Bacillus cereus*', *Pediatrics in Review*, **34**(4), pp. 196-197. https://doi.org/10.1542/pir.34-4-196
17. Sattler, S. A. *et al.* (2015). 'Characterizations of Two Bacterial Persulfide Dioxygenases of the Metallo-β-lactamase Superfamily.', *The Journal of biological chemistry*. American Society for Biochemistry and Molecular Biology Inc., **290**(31), pp. 18914-23. https://doi.org/10.1074/jbc.M115.652537
18. Spallarossa, A. *et al.* (2001). *Escherichia coli* GlpE is a prototype sulfurtransferase for the single-domain rhodanese homology superfamily, *Structure*, **9**(11), pp. 1117-1125. https://doi.org/10.1016/S0969-2126(01)00666-9
19. Tallent, S. M., Hait, J. M. and Bennett, R. W. (2015). 'Analysis of *Bacillus cereus* toxicity using PCR, ELISA and a lateral flow device', *Journal of Applied Microbiology*, **118**(4), pp. 1068-1075. https://doi.org/10.1111/jam.12766
20. Thakur, V. and Kumar, P. (2018). 'Analysis of *Hepatitis* E virus (HEV) X-domain structural model', *Bioinformation*. Biomedical Informatics, **14**(07), pp. 398-403. https://doi.org/10.6026/97320630014398
21. Uddin M. E., Ahmad T., and Ahammed T. (2017). Thermotolerant extracellular proteases produced by *Bacillus subtilis* isolated from local soil that representing industrial applications. *J. of Pure and Applied Microbiol*. **11**(2), 733-741. https://doi.org/10.22207/JPAM.11.2.12
22. Wiederstein, M. and Sippl, M.J. (2007). ProSA-web: interactive web service for the recognition of errors in three-dimensional structures of proteins. *Nucleic acids research*, **35**(suppl_2), pp.W407-W410.
23. Webb, B. and Sali, A. (2016). 'Comparative Protein Structure Modeling Using MODELLER', *Current Protocols in Protein Science*. Blackwell Publishing Inc., **86**(1), pp. 2.9.1-2.9.37. https://doi.org/10.1002/cpps.20
24. Zimmermann, L. *et al.* (2018). 'A Completely Reimplemented MPI Bioinformatics Toolkit with a New HHpred Server at its Core', *Journal of Molecular Biology*. Academic Press, **430**(15), pp. 2237-2243. https://doi.org/10.1016/j.jmb.2017.12.007

Citation: Saikat ASM, and Khalipha ABR. (2020). Structure prediction, characterization, and functional annotation of uncharacterized protein BCRIVMBC126_02492 of *Bacillus cereus*: an *in silico* approach. *Am. J. Pure Appl. Sci.*, **2**(4), 104-111. https://doi.org/10.34104/ajpab.020.01040111